Taylor & Francis
Taylor & Francis Group

Canadian Metallurgical Quarterly

The Canadian Journal of Metallurgy and Materials Science

ISSN: 0008-4433 (Print) 1879-1395 (Online) Journal homepage: www.tandfonline.com/journals/ycmq20

Investigation of dissolution kinetics of colemanite in propionic acid solutions

Mücahit Uğur, Ahmet Yartaşı, Özkan Küçük & Mehmet Muhtar Kocakerim

To cite this article: Mücahit Uğur, Ahmet Yartaşı, Özkan Küçük & Mehmet Muhtar Kocakerim (2025) Investigation of dissolution kinetics of colemanite in propionic acid solutions, Canadian Metallurgical Quarterly, 64:4, 2296-2312, DOI: 10.1080/00084433.2024.2415259

To link to this article: https://doi.org/10.1080/00084433.2024.2415259

CANADIAN METALLURGICAL QUARTERLY
2025, VOL. 64, NO. 4, 2296–2312
https://doi.org/10.1080/00084433.2024.2415259

Investigation of dissolution kinetics of colemanite in propionic acid solutions

Mücahit Uğur[a], Ahmet Yartaşı[a], Özkan Küçük[b] and Mehmet Muhtar Kocakerim[a]

[a]Department of Chemical Engineering, Faculty of Engineering, Çankırı Karatekin University, Çankırı, Turkey; [b]Department of Metallurgy and Materials Engineering, Faculty of Engineering, Bilecik Şeyh Edebali University, Bilecik, Turkey

ABSTRACT

Colemanite is one of the raw materials used to produce boron compounds which have a constituent of the richest composition ratio boron trioxide (B_2O_3). The main purpose of this study is to investigate the dissolution kinetics of colemanite in a propionic acid solution. Reaction temperature, solid–liquid ratio, propionic acid concentration, stirring speed, and particle size were chosen as relevant parameters in the dissolution. According to the results of the study, the dissolution rate was directly proportional to the rise in the reaction temperature and inversely proportional to the increase in the solid–liquid ratio, acid concentration, and particle size. Additionally, it was observed that stirring speed did not significantly effect. Experiment results were correlated with the use of the Statistica10 software programme for linear regression. For the dissolution kinetics of colemanite, a model that can control the reaction was obtained by using homogeneous and heterogeneous reaction models. It was determined that the dissolution rate of the process was controlled by diffusion through the product film (ash) and the Activation energy was calculated as 37.51 $kJ.mol^{-1}$. Experimental data were analyzed with graphical and statistical methods, and a semi-empirical mathematical model was determined, which included the parameters of the study.

La colémanite est l'une des matières premières utilisées pour la production de composés de bore qui ont un constituant du rapport de composition le plus riche en trioxyde de bore (B_2O_3). Le principal objectif de cette étude est d'examiner la cinétique de dissolution de la colémanite dans une solution d'acide propionique. On a choisi la température de réaction, le rapport solide-liquide, la concentration en acide propionique, la vitesse d'agitation et la taille des particules comme paramètres pertinents dans la dissolution. D'après les résultats de l'étude, le taux de dissolution était directement proportionnel à l'élévation de la température de réaction et inversement proportionnel à l'augmentation du rapport solide-liquide, de la concentration en acide et de la taille des particules. De plus, on a observé que la vitesse d'agitation n'avait pas d'effet significatif. Dans la production d'acide borique en utilisant l'acide propionique à partir de la colémanite, le propionate de calcium, un sous-produit, est utilisé comme agent de conservation dans l'industrie alimentaire, rendant ce procédé plus avantageux. On a corrélé les résultats expérimentaux grâce à l'utilisation du logiciel Statistica10 pour la régression linéaire. Pour la cinétique de dissolution de la colémanite, on a obtenu un modèle qui peut contrôler la réaction en utilisant des modèles de réaction homogènes et hétérogènes. On a déterminé que le taux de dissolution du procédé était contrôlé par la diffusion à travers le film de produit (cendres) et l'on a calculé l'énergie d'activation à 37.51 $kJ{\cdot}mol^{-1}$. On a analysé les données expérimentales à l'aide de méthodes graphiques et statistiques, et l'on a déterminé un modèle mathématique semi-empirique, qui incluait les paramètres de l'étude.

ARTICLE HISTORY
Received 9 May 2024
Accepted 30 September 2024

KEYWORDS
Colemanite; propionic acid; dissolution kinetics; heterogeneous reaction; activation energy

Nomenclature

X	Fractional Conversion
t	Reaction time (min)
T	Reaction temperature (K)
s	Solid amount (g)
C	Propionic acid concentration (M)
L	Liquid amount (mL)
D	Average particle size (μm, in diameter)
W	Stirring speed (rpm)
R	Universal gas constant (8.314 $j.mol^{-1}K^{-1}$)
r	Regression coefficient
k	reaction rate constant
A	Frequency factor
a, b, d, g	Model constants

İndexes

s	Solid
aq	aqueous solution
l	Liquid

CONTACT Mücahit Uğur m.ugur@karatekin.edu.tr Department of Chemical Engineering, Faculty of Engineering, Çankırı Karatekin University, Çankırı 18100, Turkey

1. Introduction

It is a critical underground resource of Turkey, which has 72% of the world's boron reserves [1]. The most important boron compounds of commercial importance in Turkey, in terms of the reserve, are colemanite ($2CaO.3B_2O_3.5H_2O$), tincal ($Na_2O.2B_2O_3.10H_2O$), ulexite ($Na_2O_2CaO_5B_2O_316H_2O$), and kernite ($Na_2B_4O_74H_2O$), respectively [2, 3]. Colemanite which has a monoclinic crystal structure, is one of the most common boron compounds. Colemanite ore which is used to produce boric acid extensively is mined in Emet-Kütahya, Bigadiç-Balıkesir, and Kestelekte-Bursa regions in Turkey [4].

Boron and its compounds are used extensively in industrial sectors such as the glass and ceramics industry, detergent and cosmetics industry, metallurgy, and agriculture. The group of boron compounds, which has small but high-value markets and makes up about one-fifth of the boron market, is also applied in abrasives, nuclear power reactors, composite materials, pharmaceuticals, catalysts, electronic components, flame retardants, wood preservatives, pulp bleaching, metal surface cleaning [5].

Boric acid, one of the most consumed boron compounds is obtained industrially from the reaction of colemanite ore with sulfuric acid. Sulfuric acid dissolves not only colemanite, but also other minerals containing calcium, magnesium, and sulfate, and the final product includes impurities. This situation causes quality and yield loss in the production of pure boric acid. In addition, boro gypsum (gypsum) formed as a by-product is stored in huge sprawling waste ponds, causing soil and environmental pollution [6]. To minimise these problems, it would be more appropriate to use weakly acidic solutions [7].

Investigating the dissolution of colemanite ore in different acidic gas and solution environments contributes to the production of various boron compounds and these studies are widely covered in the literature. Özmetin et al. investigated the dissolution kinetics of colemanite ore in acetic acid solutions and a semi-empirical kinetic model was derived. They found that the dissolution rate increased at acid concentrations up to 3.36 M, but decreased at larger concentrations, the process rate followed the first-order homogeneous reaction model and the activation energy was calculated as 51.49 $kcal.mol^{-1}$ [8]. Ceyhun et al. in a study conducted, the dissolution kinetics and mechanism of colemanite in chlorine-saturated water were investigated. In the experiments, solid/liquid ratio, particle size, mixing speed, and temperature were selected as parameters. It was observed that the fraction of minerals that reacted increased with the increase in reaction temperature and grain size and the decrease in solid/liquid ratio. Mixing speed did not affect dissolution. It was determined that the dissolution kinetics was controlled by chemical reaction, and the activation energy of dissolution was calculated as 35.56 $kJ.mol^{-1}$ [9]. Temur et al. examined the kinetics and mechanism of colemanite ore in phosphoric acid solution and determined that the dissolution rate increased with decreasing particle size and solid/liquid ratio and increasing reaction temperature, but stirring speed had no effect. They stated that the dissolution rate increased in the concentration range of 1.43-19.52 wt% and tended to decrease above this value. Likewise, the activation energy of the process whose rate is controlled by the chemical reaction was found as 53.91 $kcal.mol^{-1}$ [10]. Okur et al. investigated the dissolution kinetics of colemanite in sulfuric acid solution both in the presence and absence of ultrasound. They defined that the reaction rate fitted the Avrami model and the activation energy was 30 $kJ.mol^{-1}$ [11]. Alkan and Doğan investigated the dissolution kinetics of colemanite ore in an aqueous oxalic acid solution in the batch reactor. They determined that while the dissolution rate increases positively up to 250 $mol.m^{-3}$acid concentrations, it has a negative effect at higher acid concentrations, the dissolution rate was controlled by the diffusion from the product film and the activation energy value was calculated as 9.5 $kcal.mol^{-1}$ [12]. In a study conducted by Çavuş and Kuşlu, kinetic modelling of the dissolution of colemanite in citric acid was investigated in both mechanical shaking (ME) and microwave (MW) systems. It was observed that the dissolution rate of colemanite increased with increasing temperature, decreasing particle size, and solid/liquid ratio. In addition, calcium citrate was obtained by reacting with boric acid as a by-product. It was determined that dissolution was controlled by diffusion through the product layer. The activation energy was calculated as 28.65 and 21.08 $kJ.mol^{-1}$ for ME and MW experimental systems, respectively [13]. Kurtbaş et al. investigating dissolution kinetics of colemanite mineral in a boric acid solution saturated with SO_2 gas, determined that the reaction temperature significantly increased the dissolution rate and the activation energy was calculated as 50.15 $kcal.mol^{-1}$ [14]. Tunç et al. examined the dissolution kinetics of the reaction between colemanite and ammonium sulfate. They determined that the temperature and acid concentration had a positive effect on the dissolution rate, while the particle size and solid/liquid ratio had a negative effect, the reaction rate was controlled by the chemical reaction and the activation energy was found to be 40.46 $kcal.mol^{-1}$ [1]. Gür studied the dissolution mechanism of colemanite ore in sulfuric acid solutions and compared it with that of other strong acids. He discovered that there was an

inverse relationship between the SO_4^{2-} ion passing into the solution from colemanite ore and the H_3O^+ ion coming from the acid [15]. Guliyev et al. studied the dissolution kinetics of colemanite in ammonium hydrogen sulfate solution and an alternative reagent for boric acid production was tried to be determined. They found that the dissolution rate of the reaction was controlled by diffusion through the product film and the activation energy was calculated as 32.66 $kcal.mol^{-1}$ [7]. Künkul et al. investigated the dissolution of calcined and uncalcined colemanite ore in an aqueous ammonium carbonate solution. It was observed that the dissolution rate of calcined colemanite was higher and the calcination temperature increased up to 450°C was effective, but the effect did not change at higher temperatures. It was defined that the reaction model of the process was controlled by a first-order homogeneous model [16]. Gür and Alkan studied the dissolution kinetics of colemanite ore in perchloric acid solutions. It was found that the dissolution rate of colemanite increased as the particle size and solid/liquid ratio decreased, and the reaction temperature and acid concentration increased, but it was not affected by the stirring speed. Experimental data and mathematical modelling were performed according to heterogeneous reaction models using graphical and statistical methods and it was determined that the dissolution rate was controlled by chemical reactions. The activation energy of this process was calculated as 46.475 $kJ.mol^{-1}$ [17]. Bayca et al. investigated the dissolution kinetics of colemanite waste in an aqueous oxalic acid medium. They observed that the most effective parameter on dissolution was temperature and reaction time, but acid concentration and stirring speed did not have a significant effect [18]. Kızılca and Çopur investigated the effect of methanol on the dissolution of colemanite in a pressurised reactor environment. They determined that the dissolution rate increased with the increased temperature and pressure of the reaction and the dissolution rate decreased with the increase in particle size and solid/liquid ratio [19]. Karagöz and Kuşlu dissolved colemanite in a potassium hydrogen sulfate solution. They found that the reaction rate fits the chemical reaction-controlled model and the activation energy is 41.88 $kJ.mol^{-1}$ [20]. Sis et al. investigated the dissolution kinetics of colemanite ore in the hydrochloric acid medium and they determined that the reaction rate was controlled by the Avrami model [21]. Demir et al. in this study, the kinetic model of the dissolution of colemanite in gluconic acid solutions was carried out in a batch reactor. The dissolution rate of colemanite increases with the increase of temperature and acid concentration, particle size, and solid/liquid ratio decrease. In the kinetic evaluation, kinetic models for heterogeneous solid–liquid reactions were used together with the dissolution data. The dissolution of colemanite in gluconic acid solutions was controlled by diffusion through the product layer and the activation energy was found to be 8.39 $kJ.mol^{-1}$ [22]. In this study, Uğur 2024 investigated the dissolution of colemanite in a propionic acid solution saturated with pyrite roasting gas. The dissolution rate increases with acid concentration, gas flow rate, and increasing reaction temperature and decreases with decreasing particle size and solid-to-liquid ratio. Compared to these parameters, the stirring speed had no significant effect on the dissolution rate. It was determined that the dissolution of the process complies with the modified Avrami model. The activation energy was calculated as 38.66 $kJ.mol^{-1}$ [23].

In a study by Taylan et al. the effect of ultrasound on the dissolution of colemanite in H_2SO_4 solution and the effect of precipitated gypsum was investigated. The experiments were carried out with and without ultrasound at 85 °C and 600 and 800 rpm stirring speeds. It was determined that the effect of ultrasound increased the dissolution of colemanite and the precipitation rate of gypsum in the solution after 1 hour. It was determined that the dissolution rate increased with decreasing particle size both in the presence of ultrasound and in the absence of ultrasound. It was determined that the use of ultrasound could be a preferred method in boric acid production [24]. In a study by Bulutçu et al. they examined the formation of $MgSO_4$ impurities due to the partial decomposition of clay minerals, which is the main problem in boric acid production from colemanite ore, and the control of impurities. To obtain a product with high yield and purity, the dissolution of colemanite ore was achieved with a mixture of propionic acid and H_2SO_4 which does not decompose clay minerals. It was determined that the magnesium ratio decreased as the propionic acid ratio in the mixture increased. In this case, it was determined that the reaction time increased, but the level of soluble impurities in the strong boric acid solution decreased [25]. In a study by Kuşkay and Bulutçu, boric acid production is aimed at three different processes in the presence of propionic acid and calcium propionate. It was stated that calcium propionate in the solution has a significant effect on the solubility of boric acid, and calcium borate precipitation was detected at 75 ∘C. According to the conductivity results, it was determined that the calcium propionate concentration in the production solution should be lower than 3% to prevent any precipitation. According to the pH values, it was determined that the process should be carried out without free sulfuric acid, and the pH in the first reactor should be at 4.3 and 3.7 to form a calcium propionate concentration of 1.26% and 2.24%, respectively [26].

Table 1. Chemical analysis of colemanite ore.

Component	B_2O_3	CaO	H_2O	MgO	Moisture	Others
%	34,21	19,24	14,66	1,72	0,71	29,46

This study aims to investigate the dissolution kinetics of colemanite using a propionic acid solution which has a minimum value of industrially undesirable impurities as an alternative reagent for the production of boric acid. Therefore, the environmental pollution caused by boro gypsum, a by-product of producing boric acid from colemanite by sulfuric acid, waste, which causes environmental pollution, can be prevented.

Calcium propionate $[Ca(CH_3CH_2COO)_2]$ is formed as a by-product in the production of boric acid with propionic acid and colemanite. Calcium propionate, which has commercial value, is widely used both as a preservative additive in bakeries and bread and in the food industry to protect from bacteria and fungi [27]. In this way, calcium propionate, which is a commercially valuable by-product of our process, will be obtained.

2. Material and method

2.1. Material

The colemanite ore used in the study was obtained from the deposits in the Emet-Kütahya-Turkey region of the General Directorate of Eti Mine Works. After grinding the ore with a laboratory grinder (Restch A-5200 brand Sıeve Shaker device), it was sieved with ASTM E11 standard sieves to obtain particle size fractions of +100-150, + 150-250, + 250-400, and +400-600 µm diameter. In the kinetic calculations, the arithmetic means of the lower and upper limits of the particle sizes given as intervals were used. The chemical composition of the colemanite ore was determined by spectrophotometric and gravimetric methods, and the result of the chemical analysis is given in Table 1.

The SEM-EDX device operates with a 129 keV EDAX detector that can operate at variable high vacuum in the range of 10 - 133 Pa and a Schottky thermal field emission gun with an acceleration voltage range of 0.02 - 30 kV. It is an electron microscope that obtains images by scanning the sample surface with a focused electron beam. Electrons interact with atoms in the sample to produce different signals that contain information about the topography and composition of the sample surface. Scanning electron microscope-energy dispersive X-ray (SEM-EDX) analyses were analyzed with a Carl Zeiss brand Sigma 300 VP model device at Çankırı Karatekin University Central Research Laboratory Application and Research Center (ÇANKAM). The microstructural properties of the solid residue remaining at the end of the experiment with colemanite ore were determined by microanalysis in 3D. SEM-EDX analysis of colemanite is given in Figure 1. Raw colemanite ore has a non-porous structure. Colemanite contains dolomite mineral and illite, a clay mineral. The proportional distribution of colemanite determined by EDX analysis was determined as 11.36% B, 53.21% O, 8.78% Ca, 10.90% C, 2.71% Mg, 2.88% Al, 8.04% Si, and 2.13% K.

The X-ray diffraction method (XRD) is a technique used to determine the crystallographic structure of the material and the arrangement of atoms within the structure based on the arrangement of atoms belonging to each crystal phase. It is based on the principle of diffraction of X-rays in a characteristic regular structure in the scanning range of $10^o \leq 2\Theta \leq 90^o$. XRD analyses of colemanite ore used in this study and the solid residue formed during the reaction were performed with a Bruker brand D8 Discover model X-ray diffraction device in Bayburt Central Research Laboratory. The XRD analysis result of colemanite is given in Figure 2. In the XRD analysis, all peaks belonging to minerals other than colemanite are indicated in the figure.

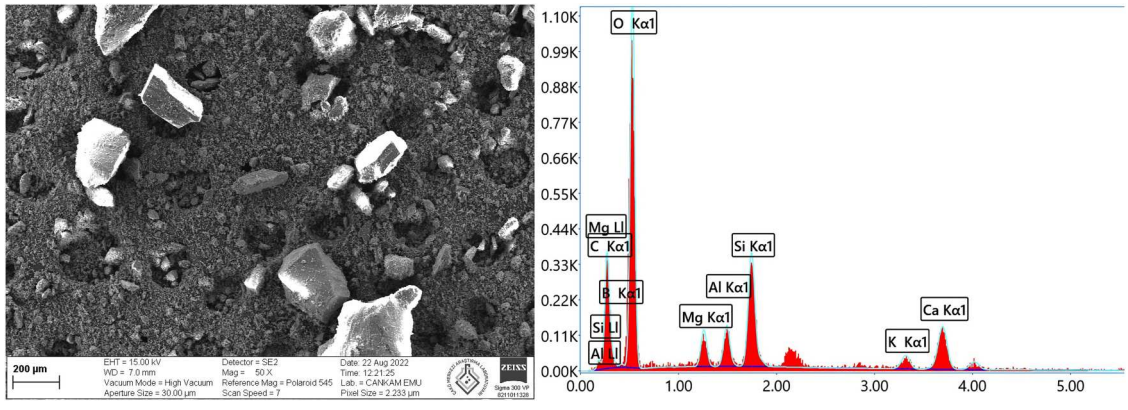

Figure 1. SEM-EDX image of colemanite ore used in the study.

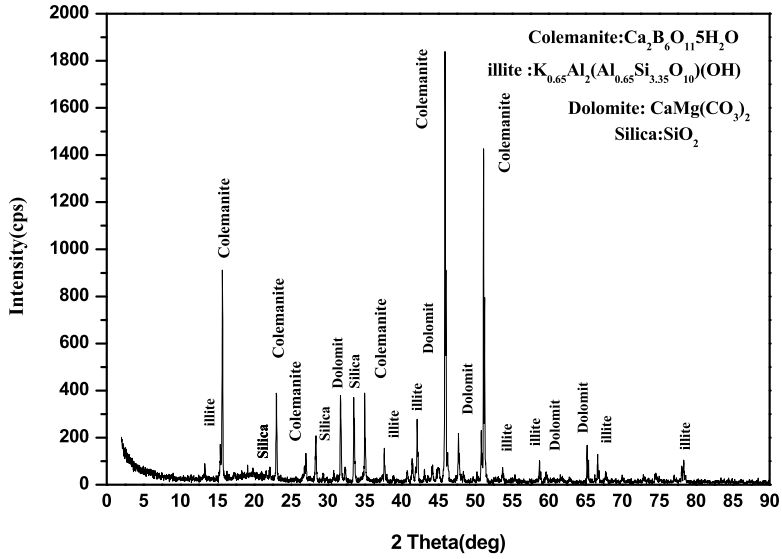

Figure 2. XRD analysis of the original colemanite ore used in the study.

Propionic acid, mannitol, and sodium hydroxide used in this study were 99% pure and supplied by Merck Millipore.

The acid constant of propionic acid, which shows weak acidity, is $1.34*10^{-5}$. Compared to the other acids used to dissolve colemanite, propionic acid has a boiling point of approximately 141°C and allows it to work at high temperatures, making it an alternative reactant in boric acid production. In addition to Ca^{2+}colemanite, there are dolomite ($CaCO_3$, $MgCO_3$), calcite ($CaCO_3$), magnesite ($MgCO_3$), and clayey structures as sources of Ca^{2+} and Mg^{2+} in the ore. Since propionic acid is not as strong as sulfuric acid, it cannot completely dissolve the main sources of impurities in colemanite and this feature is an important advantage for the production of higher-purity boric acid. Thus, this acid may be considered feasible as it does not impose an extra cost to remove the impurity in the product.

2.2. Method

In the experimental procedure; reaction temperature (K), solid/liquid ratio (S/L), propionic acid concentration (C), stirring speed (W), and particle size (D) were selected as parameters. To more clearly determine the effect of a parameter on the dissolution kinetics, the levels of the other parameters indicated with an asterisk were kept constant.

Table 2. Parameters and their ranges.

Parameters	Values
Reaction temperature, (K)	283, 293, 303*, 313, 323
Solid/liquid ratio, (S/L)	20, 40*, 60, 80
Acid concentration, (M)	4.05, 5.4*, 6.75, 8.1
Stirring speed, (rpm)	300, 400*, 500
Particle size, (μm)	100-150, 150-250, 250-400*, 400–600

* Fixed levels for each parameter

These fixed levels were determined between the maximum and minimum values. The parameters and their levels are determined as a result of preliminary experiments and literature research are given in Table 2.

2.3. Experimental procedure

The dissolution experiments were carried out in a 500 ml double-walled glass reactor under atmospheric pressure conditions. All solutions used in the experiments were prepared from analytical-grade chemicals and distilled water. A constant temperature circulator (Polyscience SD20R-30 A12E model device) was used in combination to keep the at a constant temperature suspension mixture in the reactor and a mechanical stirrer (SCILOGEX OS20-Pro model device) was used to obtain a homogeneous suspension. The experimental setup used in the study is given in Figure 3.

In the experiments, after the propionic acid solution of a certain concentration taken into the reactor was brought to the desired temperature, a certain amount of colemanite ore was added to the reactor content being stirred and the experiment was continued for a certain time. Each experiment was repeated twice and kinetic calculations were made according to the arithmetical value. After each experiment, the reactor content was filtered with a double-walled Buchner funnel using blue band filter paper. XRD and SEM analysis were performed in the dried solid residues and chemical analysis in the solutions.

2.4. Analysis, calculations, and modelling

B_2O_3 amounts were determined with the potentiometric (titrimetric) method used by [1] in 2 mL of samples

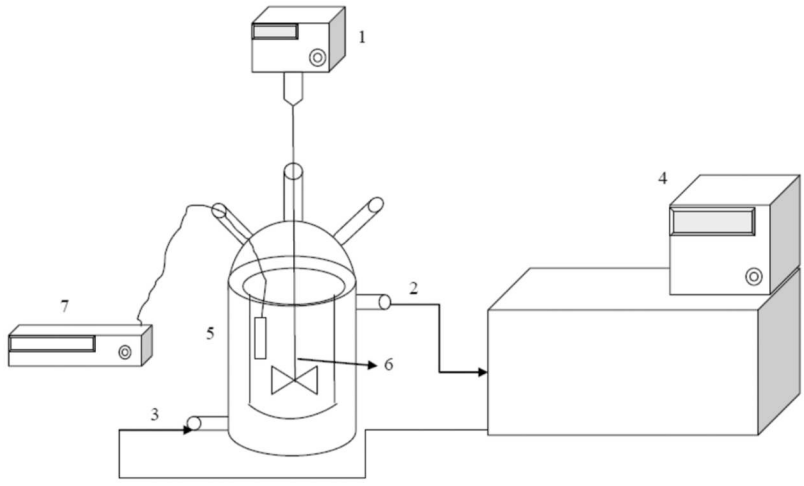

Figure 3. Experimental system used in the dissolution process. 1. Mechanical stirrer 2. Water output 3. Water input 4. Constant temperature circulator 5. Double-walled glass reactor 6. Shaft with propeller 7. pH metre.

taken from reactor content at certain time intervals. Then, the dissolution percentage of colemanite was calculated as follows.

$$X = \frac{Amount\ of\ B_2O_3\ passing\ into\ solution\ from\ colemanite\ sample\ (g)}{Amount\ of\ B_2O_3\ in\ colemanite\ sample (g)} * 100 \quad (1)$$

The dissolution percentages obtained were used to generate dissolution percentages versus time plots for kinetic modelling. The r^2 values and the kinetic model of the process are determined by the Statistica programme, which works according to the simultaneous regression model.

3. Results and discussion

3.1. Dissolution reactions

Propionic acid ionises in an aqueous medium as follows

$$4CH_3CH_2COOH_{(aq)} + 4H_2O_{(l)} \rightarrow 4CH_3CH_2COO^-_{(aq)} + 4H_3O^+_{(aq)} \quad (2)$$

The reactions that occur when colemanite is added to the propionic acid solution are as follows;

$$2CaO.3B_2O_3.5H_2O_{(s)} + 2H_3O^+_{(aq)} \rightarrow Ca^{2+}_{(aq)} + CaO.B_2O_{3\ (s,aq)} + 4H_3BO_{3\ (aq)} + 2H_2O_{(l)} \quad (3)$$

$$CaO.B_2O_{3(s,aq)} + 2H_3O^+_{(aq)} \rightarrow Ca^{2+}_{(aq)} + 2H_3BO_{3(aq)} \quad (4)$$

The total reaction is as follows;

$$2CaO.3B_2O_3.5H_2O_{(s)} + 4CH_3CH_2COOH_{(aq)} + 2H_2O \rightarrow 6H_3BO_{3(aq)} + 2Ca^{2+}_{(aq)} + 4CH_3CH_2COO^-_{(aq)} \quad (5)$$

The X-ray radiation diffraction and SEM image of the solid residue obtained in the experimental study are given in Figures 4 and 5, respectively. It is observed that in the dissolution of colemanite ore, calcite ($CaCO_3$), magnesite ($MgCO_3$), and clay minerals coming from colemanite ore, remain in the solid residue, and they form a layer called the 'product layer'. Likewise, the walk of the dissolution process is given schematically in Figure 6.

3.2. Mechanism of the dissolution process

Colemanite ore is not found in a pure form. The ore contains clay and carbonate minerals such as calcite, magnesite, and dolomite. According to the analysis results given in Table 1, the ore contains 67.12% colemanite, ~10 carbonate minerals, ~22.17 clay minerals and, 0.71% moisture. Although the clay minerals also contain Ca^{2+} and Mg^{2+}, the amount of Ca^{2+} and Mg^{2+} passing from the clay minerals to the solution was thought to be negligible under the studied conditions. It has been observed that the amounts of Ca^{2+} and Mg^{2+} passing from the carbonate minerals to the solution vary between 0.20 and 0.40% in the ore depending on the parameters. Therefore, carbonate minerals and clay minerals that remain undissolved together form an 'ash layer'. Propionic acid, on the other hand, mainly gives the reactions in Equations 3 and 4 with the colemanite mineral in its structure. The reaction takes place in two stages. In the first

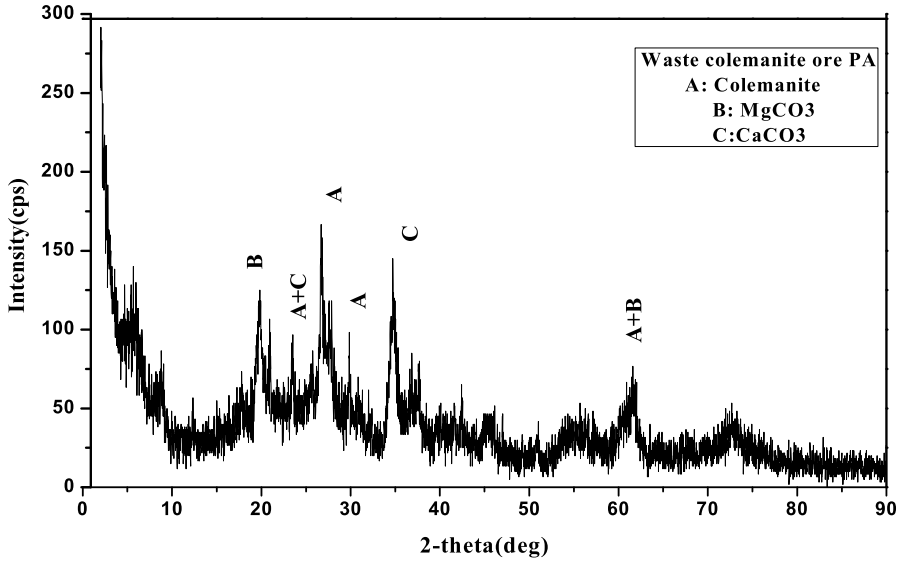

Figure 4. X-ray diffractogram of the solid residue obtained in experiments.

stage, the products are boric acid and $CaO.B_2O_3$. In the second stage, the product is only boric acid. The dissolution rate of boric acid formed in the 1st and 2nd stages is high. However, it is stated in some publications that the formed boric acid forms a product film. However, the main product film resistance here is the $CaO.B_2O_3$ layer formed in the 1st stage. The dissolution rate of this formation is much slower than boric acid. As a result, a 'product layer' consisting of clay and carbonate minerals and a product layer of boric acid and $CaO.B_2O_3$ are formed in solution with colemanite, as seen in Figure 6, and it is thought that the reaction rate is controlled by diffusion from this product layer.

3.3. Effects of parameters

In this study, reaction temperature, solid/liquid ratio, propionic acid concentration, stirring speed, and particle size were determined as process parameters to examine the dissolution kinetics of colemanite. According to the experimental plan given in Table 3, constant working conditions in the experiments were selected as 40 $g.L^{-1}$ for solid/liquid ratio, 5.4 M for propionic acid concentration, 400 rpm for stirring speed, and 250–400 μm for particle size, and 303 K for reaction temperature.

3.4. Effect of solid–liquid ratio

The effect of the solid/liquid ratio on the dissolution rate of colemanite ore was examined for 20, 40, 60, and 80 $g.L^{-1}$ solid/liquid ratios. The results given graphically in Figure 7 show that the dissolution rate decreases with increasing the solid/liquid ratio. This situation can be explained by the decrease in the number of colemanite particles and surface area per

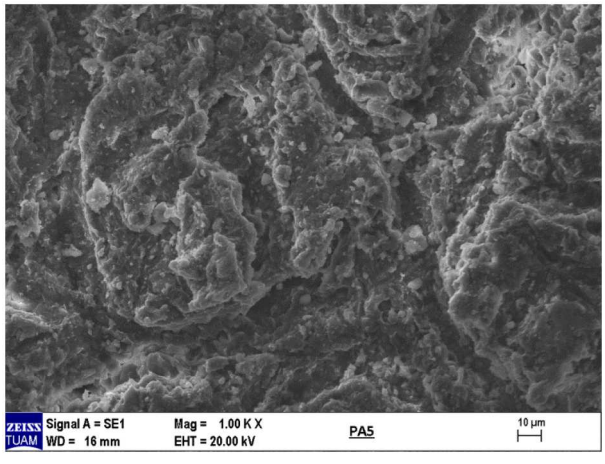

Figure 5. SEM image of the solid residue obtained in experiments.

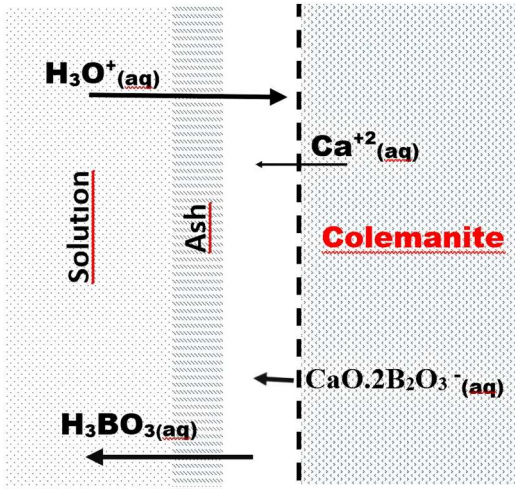

Figure 6. Schematic view of the dissolution process.

Table 3. Experimental plan used in the study.

Experiment No.	Reaction temperature (K)	Solid/liquid ratio (***S/L***)	Acid concentration (M)	Stirring rate (rpm)	Particle size (μm)
1	**283**	40	5.4	400	250–400
2	**293**	40	5.4	400	250–400
3	**303**	40	5.4	400	250–400
4	**313**	40	5.4	400	250–400
5	**323**	40	5.4	400	250–400
6	303	**20**	5.4	400	250–400
7	303	**60**	5.4	400	250–400
8	303	**80**	5.4	400	250–400
9	303	40	**4.05**	400	250–400
10	303	40	**6.75**	400	250–400
11	303	40	**8.1**	400	250–400
12	303	40	5.4	**300**	250–400
13	303	40	5.4	**500**	250–400
14	303	40	5.4	400	**100–150**
15	303	40	5.4	400	**150–250**
16	303	40	5.4	400	**400–600**

propionic acid solvent in each reaction mixture. This decreases the rate of B_2O_3 passing into the solution and increases the rate of solid retention. Similar results were observed in the dissolution of colemanite ore in methanol and ammonium hydrogen sulfate solutions [7, 19]. In contrast to the decrease in the dissolution rate, an increase in the amount of dissolved colemanite is observed [20, 28, 29]. Indeed, in Figure 7, the amounts of B_2O_3 passing into solution in the reaction medium at the 25th minute of dissolution are 1.72, 2.8, 3.8, and 4.7 g, respectively, for solid/liquid ratios of 20, 40, 60, and 80 $g.L^{-1}$.

3.5. Effect of acid concentration

The effect of propionic acid concentration on the dissolution rate of colemanite is given graphically in Figure 8 for 4.05, 5.4, 6.75, and 8.1 M propionic acid. As can be seen in this figure, the dissolution rate of colemanite decreases with increasing the acid concentration. Likewise, it is observed in Figure 8 that the compounds formed in Reactions 3 and 4, $H_3BO_{3\,(aq,s)}$ and $CaO.B_2O_{3\,(aq,s)}$, form a layer around unreacted colemanite particles. Since the effect of acid concentration is examined, the amount of colemanite used and the surface area are constant. The higher the acid concentration, the faster the

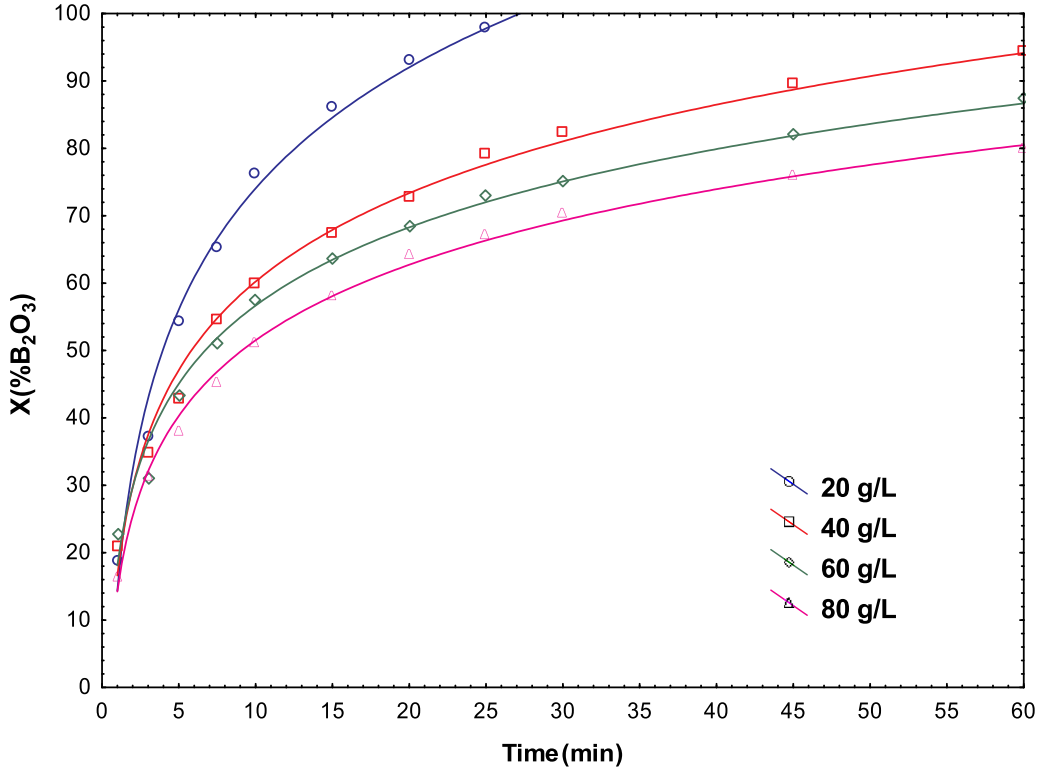

Figure 7. Effect of solid/liquid ratio on the dissolution rate of colemanite ore in propionic acid solutions.

reaction and the layer around unreacted colemanite cores becomes tighter and thicker. The layer formation slows the dissolution of colemanite. The effect of acid concentration can be explained by the fact that H_3O^+ ions form a product layer around the unreacted colemanite cores, preventing the ore from easily dissolving [30]. There is also, a layer of ash outside the product layer.

3.6. Effect of stirring speed

The effect of stirring speed on the dissolution rate of colemanite has been investigated at 300, 400, and 500 rpm due to suspension homogeneity fully achieved at a stirring speed of 300 rpm. The results are given graphically in Figure 9. According to the experimental results, it was concluded that the effect of stirring speed on the dissolution rate of colemanite can be practically ignored. Similar results for the dissolution of colemanite were found with solutions such as acetic acid [8], oxalic acid [12], and methanol [19].

To investigate the effect of particle size on dissolution rate, experiments were carried out using size ranges of +100-150, + 150-250, + 250-400, and +400-600 µm. In the graphs of the dissolution percentage versus time given in Figure 10, it can be seen that as the particle size decreases, the dissolution rate increases due to the increase in the surface area corresponding to the unit particle amount. Therefore, it is naturally expected that the dissolution rate will increase with decreasing particle size [7, 19, 29].

The effect of temperature on the dissolution rate was investigated in 283, 293, 303, 313, and 323 K. It appeared to increase the dissolution rate with an increase in the temperature as shown graphically in Figure 11, and in 30-minute trial period, the dissolution percentage of colemanite reached 99.85 at 323 K, 95.43 at 313 K, 84.96 at 303 K, 68.33 at 293 K and 40.38. The increase in the reaction rate with the increase in temperature was attributed to the increase in molecular motions and collisions in the solution [18, 28]. Thus, the amount of B_2O_3 passes to the solution and therefore, the reaction rate increases, too.

3.7. Kinetic analysis

Solid–liquid reactions are studied according to homogeneous and heterogeneous reaction rate models. The reaction rate equations for these models are given in the literature [31]. In the homogeneous reaction models, it is thought that a fluid containing the reactant penetrates every point of the particle and reacts at every point of the particle. In the heterogeneous models, it is predicted that the reactant first passes through a fluid film and then an ash or product layer and reaches the outer surface of the unreacted solid, and the reaction takes place on the surface of the unreacted solid core [12]. The products occurring on the reaction surface first pass through the ash or product layer to the fluid

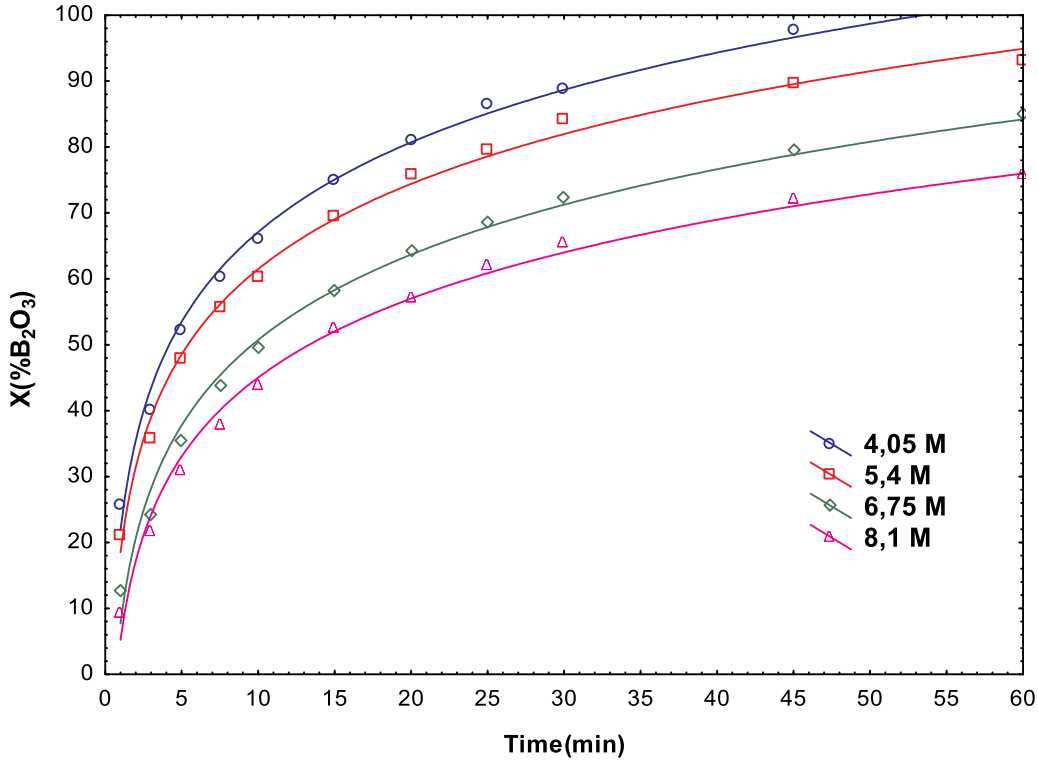

Figure 8. Effect of PA concentration on the dissolution rate of colemanite in propionic acid solutions.

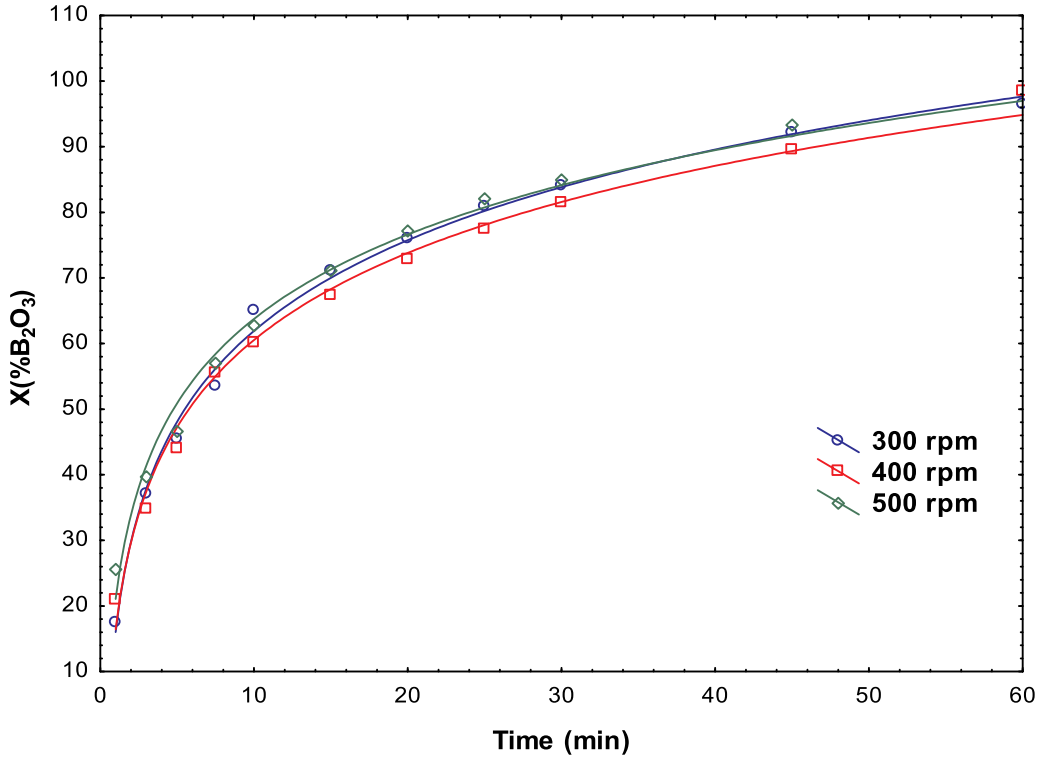

Figure 9. Effect of stirring speed on the dissolution rate of colemanite in propionic acid solutions Effect of particle size.

film and then, through the fluid film layer to the bulk of the fluid. Each of the first three steps specified for heterogeneous reactions corresponds to a resistance to the reaction, and the step with the greatest resistance controls the rate [32].

3.7.1. Determination of the kinetic model

In determining the rate control model of the process, the integrated rate equations of the control steps were tried one by one using the B_2O_3 dissolution percentages (X) for all parameters and levels, and the r^2 (regression) values were as in Table 4. Linear regression analysis, r^2 is a statistical measure used to evaluate the extent to which the independent variable explains the variability in the dependent variable in the regression model and to evaluate the performance of the model in regression analysis. It usually takes a value between 0 and 1. The closer it is to 1, the more successful the model is considered to be. The r^2 value is defined and calculated as the ratio of the explained variation (SSR) to the total variation (SST).

It was found that the diffusion through the ash layer for constant-size spherical particles, given in Equation 6, was compatible according to r^2 values in Table 4.

$$1 - 3(1 - \mathrm{X})^{2/3} + 2(1 - \mathrm{X}) = \mathrm{kt} \qquad (6)$$

The fact that the stirring speed does not affect the dissolution rate indicates as seen in Figure 9 that there is no fluid film resistance that can affect the dissolution rate [22]. The low r^2 values of integrated rate expression for diffusion through fluid film in Table 4 also verified this view.

Another indicator to predict the most appropriate rate control model is f(X) graphs versus time, which should give a straight line for each of the parameters. Graphs of f(X) versus time using obtained experimental data were plotted and only graphs of $1 - 3(1 - X)^{\frac{2}{3}} + 2(1 - X)$ versus time were found to be linear. Figures 12–16 acquired for solid–liquid ratio, propionic acid concentration, stirring speed, particle size, and reaction temperature, respectively confirm that the process rate is controlled by diffusion through the ash layer. The kinetic models used in the study for the shrinking core model are not only diffusion-controlled leaching. As can be seen from Table 4, 9 models, including chemically controlled leaching, were tested, and r^2 values were determined. As can be understood from this table, the model with the highest r^2 value belongs to diffusion-controlled leaching from the ash (product) film. In addition, it is given in the literature that processes with activation energy above 40 $kJ.mol^{-1}$ are chemically controlled, those below 20 $kJ.mol^{-1}$ are diffusion-controlled from the fluid film, and those between 20 and 40 $kJ.mol^{-1}$ are diffusion-controlled from the ash (product) film. The activation energy value of 37.51 $kJ.mol^{-1}$ also confirms that our process is diffusion-controlled from the product film (ash).

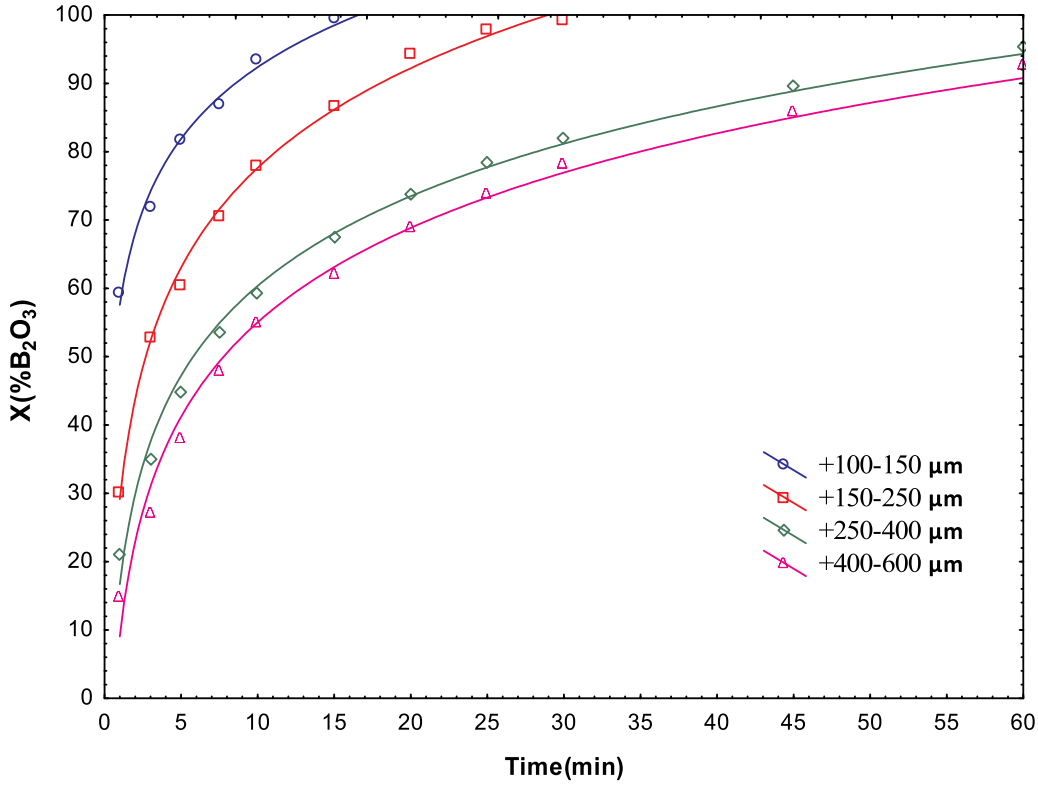

Figure 10. Effect of particle size on the dissolution rate of colemanite in propionic acid solutions Effect of temperature.

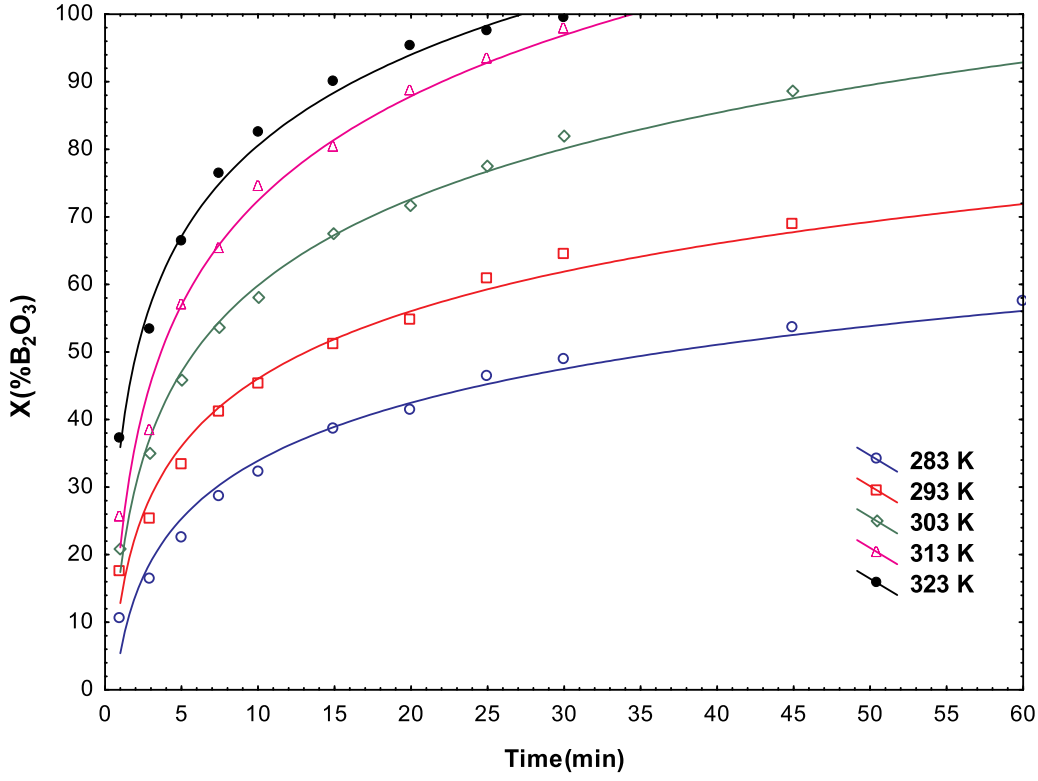

Figure 11. Effect of reaction temperature on the dissolution rate of colemanite in propionic acid solutions.

Table 4. Rate equations and regression (r^2) values tried in modelling.

Equations	Type of rate control	r^2
$\boldsymbol{kt = 1 - 3(1 - X)^{\frac{2}{3}} + 2(1 - X)}$	**Product film diffusion controlled for constant-size spherical particles**	**0,953**
$kt = 1 - (1 - X)^{1/3}$	Chemical reaction control for constant-size spheres	0,83
$kt = 1 - (1 - X)^{1/2}$	Fluid film diffusion-controlled for shrinking sphere, large grains	0,715
$kt = 1 - (1 - X)^{2/3}$	Fluid film diffusion controlled small grains for shrinking sphere	0,54
kt = -ln(1-X)	The first-order pseudo homogeneous reaction model	0,93
$kt = \frac{X}{1 - X}$	The second-order pseudo homogeneous reaction model	0,67
$kt^m = -\ln(1 - X)$	Avrami	0,950
$kt = X^2$	Product film diffusion control for constant-size flat plate	0,852
kt = X + (1-X)ln(1-X)	Product film diffusion control for constant-size cylinder	0,930

3.7.2. Determination of activation energy and Arrhenius constant

The activation energy (E_a) value of a reaction indicates the extent to which the reaction rate changes depending on the temperature. The activation energy of a chemical reaction is closely related to the reaction rate. The higher the activation energy, the slower the reaction will be. This is because molecules can only complete a reaction if the top of the activation energy limit is reached. Reactions with high activation energies are more affected by temperature changes. In other words, the change in reaction rate is much greater as the temperature increases.

In heterogeneous reactions, mass transfer should also be considered as an additional factor affecting the reaction rate. In heterogeneous reactions where ash or product film is formed, it is assumed that the particle size does not change during the reaction, but a product layer that gradually thickens is formed. It is assumed that the reactant (here H_3O^+) passes from the main fluid mass in a fluid film surrounding the ash film and then through the ash film, reaches the reaction surface and reacts on this surface. The reactant encounters resistances while passing through these films or layers and reacting on the reaction surface (fluid film resistance, ash or product layer resistance, surface chemical reaction resistance). The largest of these three resistances controls the rate of the reaction. As stated above, the activation energy is related to the surface chemical reaction. The relationship of these resistances to the reaction rate can be expressed as follows.

$$-\frac{1}{S_{ex}}\frac{dN_A}{dt} = \frac{C_A}{\frac{1}{k_g} + \frac{R}{2D_e} + \frac{3}{k}}$$

Here C_A is the fluid reactant concentration, R is the initial radius of the particle, S_{ex} is the unchanging outer surface area of the particle, dNA/dt is the number of particles reacting per unit time De is the effective diffusion coefficient of the fluid in the passage of the product or ash layer, k_g is the mass transfer coefficient between the liquid and the particle, k" is the first order rate constant for the surface reaction. Here, the first of the three terms in the denominator on the right side of the equation shows the fluid film resistance, the second shows the ash film resistance, and the third shows the surface reaction resistance. Under experimental conditions, $\frac{1}{k_g} << \frac{R}{2D_e} + \frac{3}{k}$ can be written.

Temperature is an important parameter in determining the speed control step in a process and it is associated with the activation energy using the Arrhenius equation expressed as.

$$k = A.e^{\frac{-E}{RT}} \tag{7}$$

The reaction rate constant, k, is determined from the slope of each temperature line in Figure 15. E is activation energy $J.mol^{-1}$ and R is universal gas (8.314 $j.mol^{-1}K^{-1}$) [33, 34]. Equation 8 is obtained by taking the natural logarithm of both sides of the Arrhenius equation in Equation 7.

$$\ln k = \ln A - \frac{E}{RT} \tag{8}$$

To determine the activation energy of the reaction, the – lnk values are plotted against $1/T(K)$ and determined from the slope of this graph [35]. The Arrhenius plot is shown in Figure 16.

From the slope of the line in the Arrhenius plot in Figure 16, the activation energy (E) was determined 37.51 $kJ.\ mol^{-1}$ and the Arrhenius constant (A) was determined as $3.35{*}10^4$.

The relationship of the rate constant (k) in the diffusion model through the ash layer in Equation 6 with the solid–liquid ratio, propionic acid concentration, particle size, and stirring speed is given in Equation 9.

$$k = A.(KS)^a.(C)^b.(D)^c.(W)^d.e^{-E/RT} \tag{9}$$

Equation 9 is written instead of the k rate constant in the diffusion model through the product film in Equation 6 and Equation 10 is obtained.

$$1 - 3(1 - X)^{2/3} + 2(1 - X) = A.(KS)^a.(C)^b.(D)^c.e^{-E/RT} * t \tag{10}$$

Here, the exponential constants a, b, and c were determined by statistical calculations with multiple

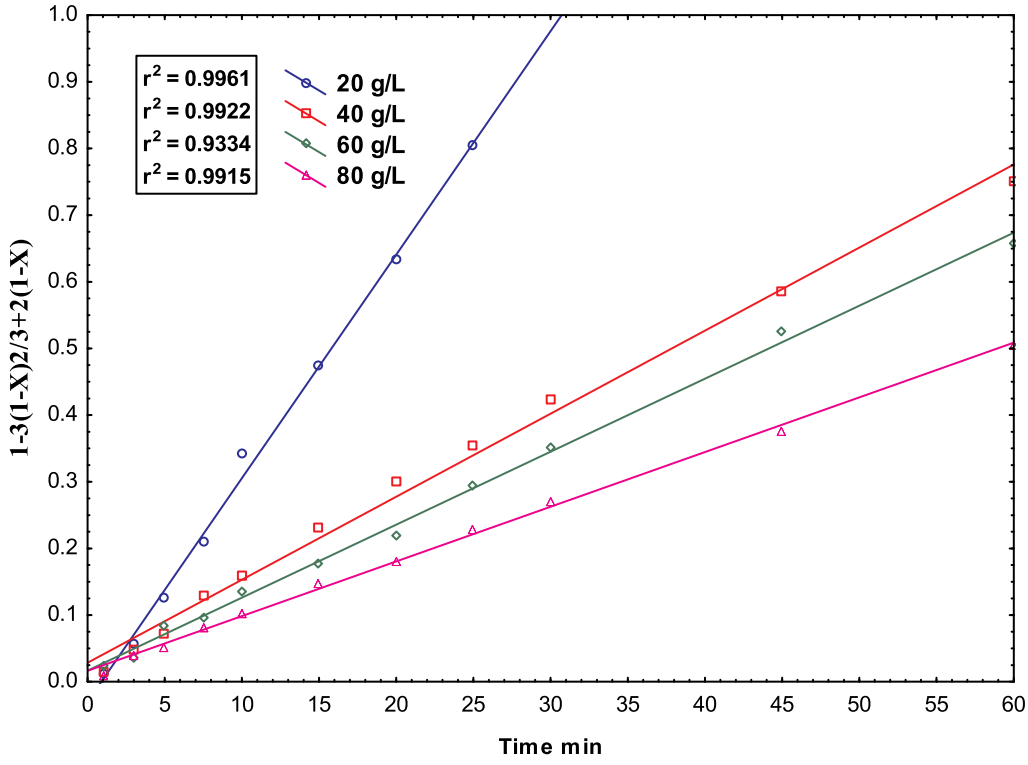

Figure 12. Variation of $1 - 3(1 - X)^{\frac{2}{3}} + 2(1 - X)$ versus time at different solid/liquid ratios.

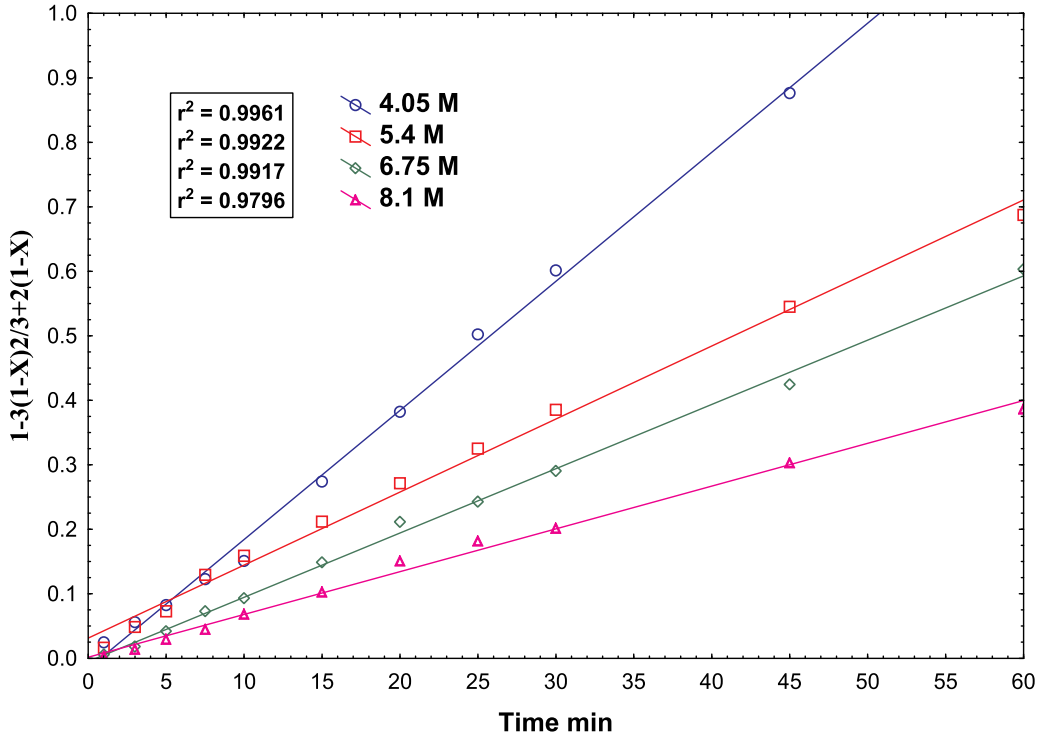

Figure 13. Variation of $1 - 3(1 - X)^{\frac{2}{3}} + 2(1 - X)$ versus time at different propionic acid ratios.

simultaneous regression using the Statistica 10 package programme. The exponential constants were calculated as – 1.10, – 1.40, and – 1.35 respectively. These constants were substituted in Equation 10 and a semi-empirical mathematical expression of the diffusion model from the product film depending on the

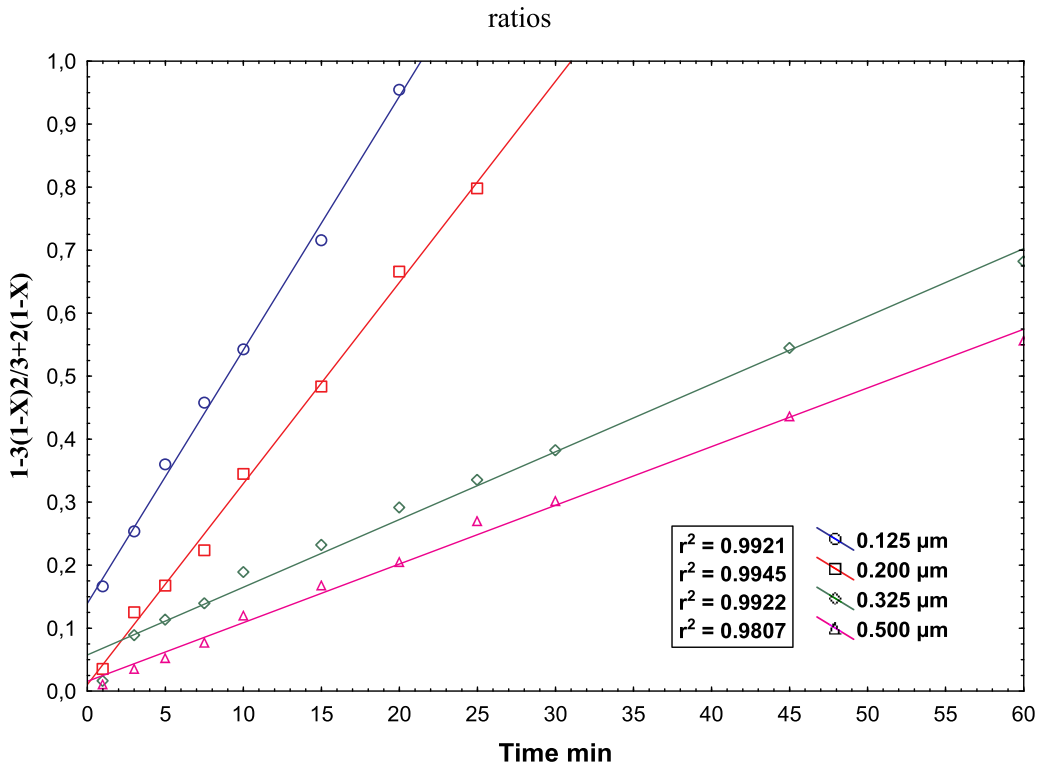

Figure 14. Variation of $1 - 3(1 - X)^{\frac{2}{3}} + 2(1 - X)$ versus time at different particle sizes.

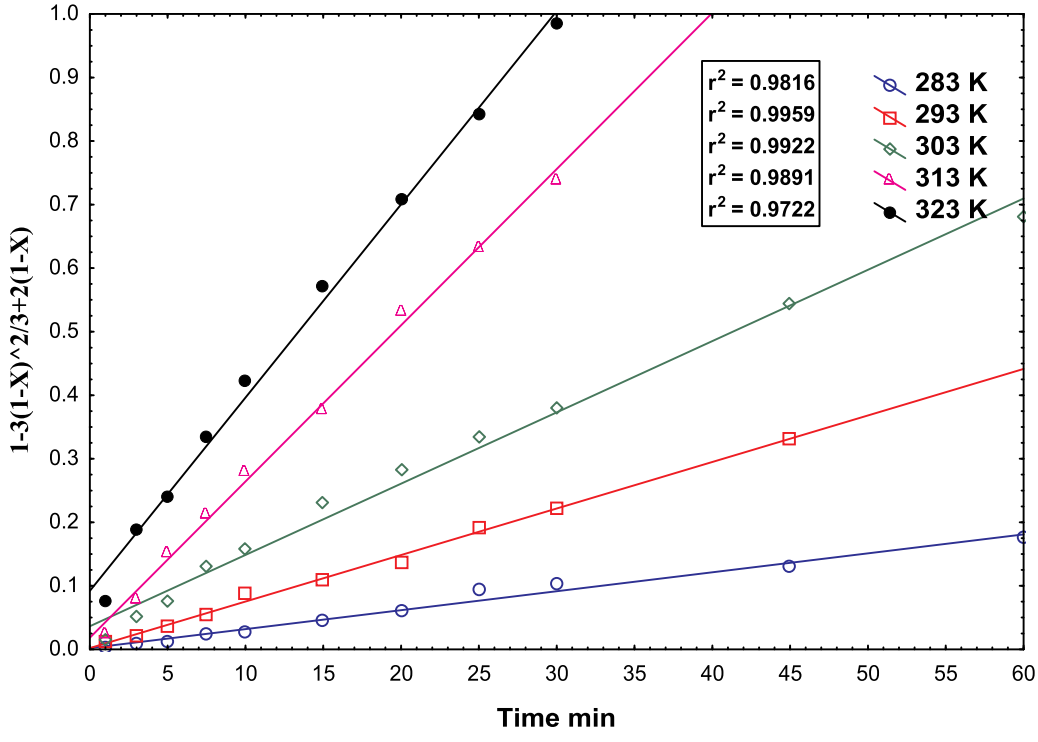

Figure 15. Variation of $1 - 3(1 - X)^{\frac{2}{3}} + 2(1 - X)$ versus time at different reaction temperatures.

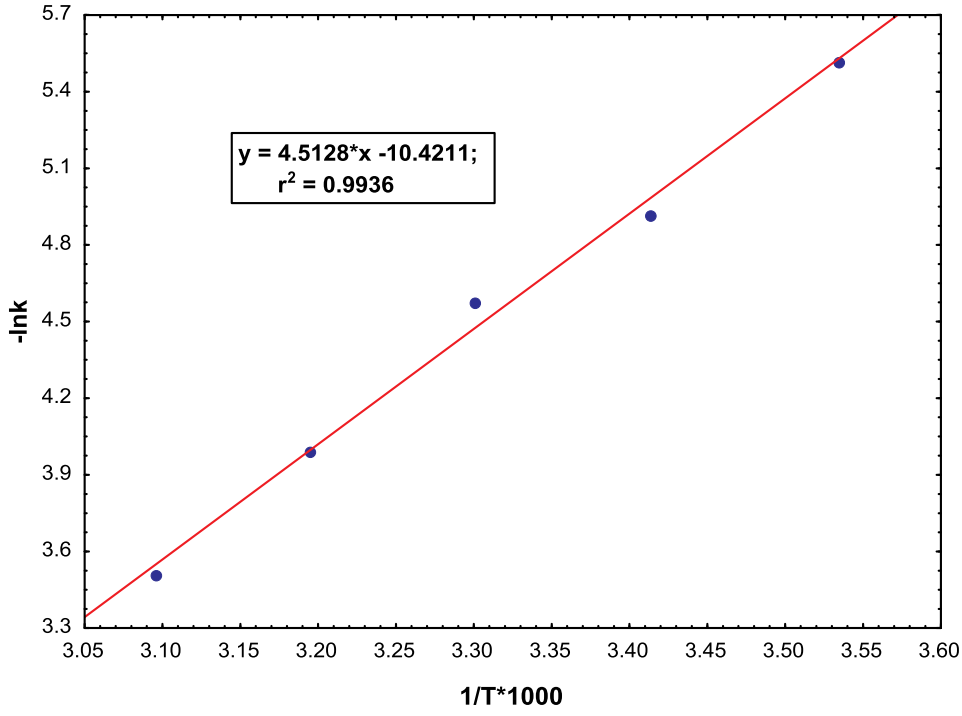

Figure 16. –lnk versus $1/T(K)*1000$ plot (Arrhenius plot).

parameters was obtained as in Equation 11.

$$1-3(1-X)^{2/3}+2(1-X) = 3.35*10^{4}.(KS)^{-1.10}.(C)^{-1.40}.(D)^{-1.35}.e^{\frac{-37.51}{R*T}}*t \quad (11)$$

3.7.3. Validation of the kinetic model

Theoretical dissolution values ($X_{\text{theoretical}}$) and experimental dissolution values ($X_{\text{experimental}}$) were determined as trial results with the help of the semi-empirical mathematical equation in Equation 11 determined for the model. $X_{\text{theoretical}}$ versus $X_{\text{experimental}}$ data were plotted in Figure 17 to determine the fit of the

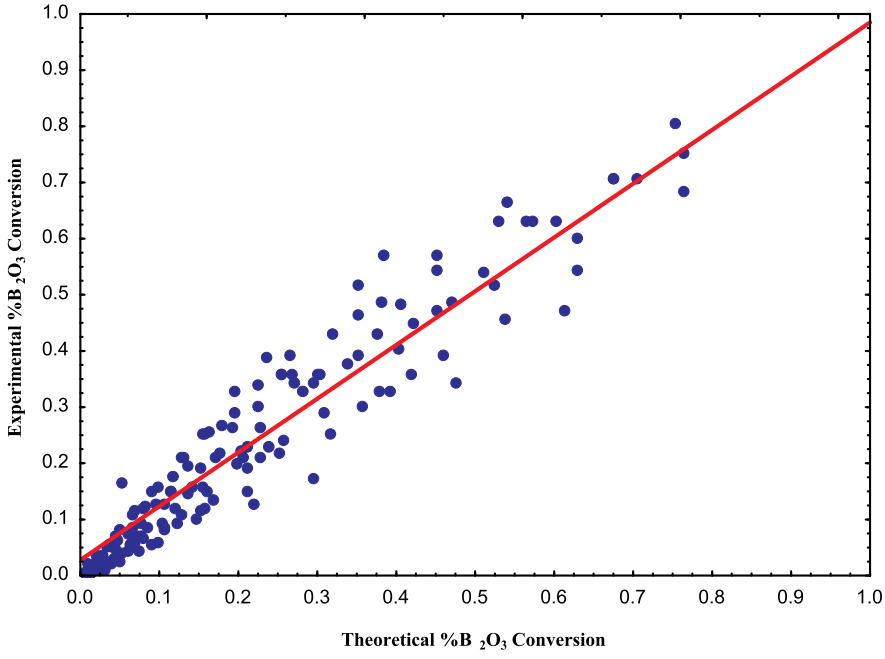

Figure 17. Comparison of experimental data and theoretical data obtained from the model.

model with the experimental data. The fact that the theoretical and experimental dissolution values are on the same diagonal on the graph shows that the chosen model is in good agreement with the experimental results.

4. Conclusions

In this study, the dissolution kinetics of colemanite in propionic acid solution in an aqueous medium at atmospheric pressure was investigated to evaluate as an alternative reactant for boric acid production. The effects of the parameters determined by the preliminary trial and literature information on the dissolution rate of colemanite were investigated. Obtained results are as follows;

- ✓ The rate of dissolution increased with increasing reaction temperature.
- ✓ The dissolution rate decreased with increasing solid–liquid ratio, propionic acid concentration, and particle size.
- ✓ We determined propionic acid, which has a weakly acidic property, can be used to dissolve colemanite ore for boric acid production. It was seen that the boric acid produced was of high purity and no environmentally harmful waste was generated.
- ✓ At fixed parameters, the B_2O_3% passing into the solution is approximately 89.6%. In these conditions, approximately 99.9% of Ca passed into the solution in the 30th minute. The highest B_2O_3% rate was determined as 99.9% in the 13th experiment with the parameters of 333 K, 20 $g.L^{-1}$ 4.05 M, and 500 rpm. In these conditions, approximately 99.9% of Ca passed into the solution in the 15th minute.
- ✓ Experimental results were used to determine the kinetics model of the dissolution of colemanite and applied to homogeneous and heterogeneous models. It was determined that the diffusion model through the product layer $[kt = 1 - 3(1 - X)^{2/3} + 2(1 - X)]$ was the most suitable. The activation energy of the process was calculated as 37.51 $kJ.mol^{-1}$.

  Considering the parameters mentioned above, the regression coefficient(r^2) of the mathematical model was calculated as 0.953.

$$1 - 3(1 - X)^{2/3} + 2(1 - X) = 3.35 * 10^4.(KS)^{-1.10}.(C)^{-1.40}.(D)^{-1.35}.e^{\frac{-37.51}{R*T}} * t$$

- ✓ In the current technology, colemanite reacts with sulfuric acid to form boric acid and unused waste borogypsum ($CaSO_4 2.H_2O$). Calcium propionate, formed as a by-product of boric acid in the proposed process, is a valuable product used as a preservative in the production of bakery products. Thus, the formation of borogypsum, an environmentally problematic product, is prevented, a valuable by-product is obtained, the cost of boric acid is reduced, and its competitiveness is increased. On the other hand, the calcium propionate to be obtained can also be used without purification. Since boric acid has an antibacterial effect, its presence in low concentrations may not pose a health risk.

Acknowledgments

Determination of the concentration of the elements was made using the Shimadzu AA-7000 Atomic Absorption Spectrophotometer (AAS) device at Çankırı Karatekin University. This research was also carried out with the support of the Scientific Research Project (MF210621D06) funded by Çankırı Karatekin University. Authors thank to Çankırı Karatekin University, Scientific Research Project Management Unit (ÇAKÜ-BAP).

Credit author statement

Mücahit Uğur: Conceptualisation, Data curation, Visualisation, Investigation, Methodology, Writing-Reviewing and Editing. Ahmet Yartaşı: Investigation, Formal analysis, Visualisation, Data curation. Özkan Küçük: Conceptualisation, Supervision, Validation, Data curation, Visualisation, Investigation, Methodology, Writing-Reviewing and Editing. Mehmet Muhtar Kocakerim: Supervision, Validation, Methodology, Writing-Reviewing and Editing, Resources.

Disclosure statement

No potential conflict of interest was reported by the author(s).

Funding

This work was supported by Çankiri Karatekin Üniversitesi: [Grant Number MF210621D06].

Data availability

Data will be made available on request.

References

[1] Tunç M, Kocakerim MM, Küçük Ö, et al. Dissolution of colemanite in $(NH_4)2SO_4$ solutions. Korean J Chem Eng. 2007;24:55–59. doi:10.1007/s11814-007-5009-0

[2] Sert H, Yıldıran H, Toscalı D. An investigation on the production of sodium metaborate dihydrate from ulexite by using trona and lime. Int J Hydrogen Energy. 2012;37:5833–5839. doi:10.1016/j.ijhydene.2012.01.012

[3] Tombal T, Özkan Ş, Kurşun Ünver İ, et al. Properties, production, uses of boron compounds and their importance in nuclear reactor technology. Boron. 2016;1:86–95.

[4] Mergen A, Demirhan M. Dissolution kinetics of probertite in boric acid solution. Int J Miner Process. 2009;90 (1-4):16–20.
[5] Kavcı E, Calban T, Colak S, et al. Leaching kinetics of ulexite in sodium hydrogen sulphate solutions. J Ind Eng Chem. 2014;20:2625–2631. doi:10.1016/j.jiec.2013.12.089
[6] Budak A, Gönen M. Extraction of boric acid from colemanite mineral by supercritical carbon dioxide. J Supercrit Fluids. 2014;92:183–189. doi:10.1016/j.supflu.2014.05.016
[7] Guliyev R, Kuşlu S, Çalban T, et al. Leaching kinetics of colemanite in ammonium hydrogen sulphate solutions. J Ind Eng Chem. 2012;18:1202–1207. doi:10.1016/j.jiec.2012.01.044
[8] Özmetin C, Kocakerim MM, Yapıcı S, et al. A semiempirical kinetic model for dissolution of colemanite in aqueous CH_3COOH solutions. Ind Eng Chem Res. 1996;35:2355–2359. doi:10.1021/ie950186o
[9] Ceyhun I, Kocakerim M, Saraç H, et al. Dissolution kinetics of colemanite in chlorine saturated water. Theor Found Chem Eng. 1999;33:253–257.
[10] Temur H, Yartaşı A, Copur M, et al. The kinetics of dissolution of colemanite in H_3PO_4 solutions. Ind Eng Chem Res. 2000;39:4114–4119. doi:10.1021/ie990647w
[11] Okur H, Tekin T, Ozer AK, et al. Effect of ultrasound on the dissolution of colemanite in H2SO4. Hydrometallurgy. 2002;67:79–86. doi:10.1016/S0304-386X(02)00137-8
[12] Alkan M, Doğan M. Dissolution kinetics of colemanite in oxalic acid solutions. Chem Eng Process. 2004;43:867–872. doi:10.1016/S0255-2701(03)00108-9
[13] Çavuş F, Kuşlu S. Dissolution kinetics of colemanite in citric acid solutions assisted by mechanical agitation and microwaves. Ind Eng Chem Res. 2005;44:8164–8170. doi:10.1021/ie050134r
[14] Kurtbaş A, Kocakerim MM, Küçük Ö, et al. Dissolution of colemanite in aqueous solutions saturated with both sulfur dioxide (SO_2) gas and boric acid. Ind Eng Chem Res. 2006;45:1857–1862. doi:10.1021/ie050050i
[15] Gür A. Dissolution mechanism of colemanite in sulphuric acid solutions. Korean J Chem Eng. 2007;24:588–591. doi:10.1007/s11814-007-0007-9
[16] Künkül A, Aslan NE, Ekmekyapar A, et al. Boric acid extraction from calcined colemanite with ammonium carbonate solutions. Ind Eng Chem Res. 2012;51:3612–3618. doi:10.1021/ie202388x
[17] Gür A, Alkan ME. Leaching kinetics of colemanite in perchloric acid solutions. J Chem Eng Jpn. 2008;41:354–360. doi:10.1252/jcej.07WE194
[18] Bayca SU, Kocan F, Abali Y. Dissolution of colemanite process waste in oxalic acid solutions. Environ Prog Sustain Energy. 2014;33:1111–1116. doi:10.1002/ep.11889
[19] Kizilca M, Copur M. Kinetic investigation of reaction between colemanite ore and methanol. Chem Eng Commun. 2015;202:1528–1534. doi:10.1080/00986445.2014.956739
[20] Karagöz Ö, Kuşlu S. Dissolution kinetics of colemanite in potassium dihydrogen phosphate solution (KH_2PO_4). Int J Hydrogen Energy. 2017;42:23250–9. doi:10.1016/j.ijhydene.2017.04.051
[21] Sis H, Bentli I, Demirkiran N, et al. Investigating dissolution of colemanite in sulfuric acid solutions by particle size measurements. Sep Sci Technol. 2019;54:1353–1362. doi:10.1080/01496395.2018.1532961
[22] Demir F, Al-Ani AOA, Lacin O. A kinetic analysis for production of calcium borogluconate from colemanite. Int J Chem Kinet. 2020;52:769–776. doi:10.1002/kin.21398
[23] Uğur M. Dissolution kinetics for colemanite ore in propionic acid solutions saturated with pyrite roasting gas. Iran J Chem Chem Eng. 2024. (Article in Press).
[24] Taylan N, Gürbüz H, Bulutcu A. Effects of ultrasound on the reaction step of boric acid production process from colemanite. Ultrason Sonochem. 2007;14:633–638. doi:10.1016/j.ultsonch.2006.11.001
[25] Bulutcu A, Ertekin C, Celikoyan MK. Impurity control in the production of boric acid from colemanite in the presence of propionic acid. Chem Eng Process. 2008;47:2270–2274. doi:10.1016/j.cep.2007.12.012
[26] Kuskay B, Bulutcu A. Design parameters of boric acid production process from colemanite ore in the presence of propionic acid. Chem Eng Process. 2011;50:377–383. doi:10.1016/j.cep.2011.02.013
[27] Phechkrajang CM, Yooyong S. Fast and simple method for semiquantitative determination of calcium propionate in bread samples. J Food Drug Anal. 2017;25:254–259. doi:10.1016/j.jfda.2016.03.013
[28] Şimşek HM, Guliyev R, Beşe AV. Dissolution kinetics of borogypsum in di-ammonium hydrogen phosphate solutions. Int J Hydrogen Energy. 2018;43:20262–20270. doi:10.1016/j.ijhydene.2018.07.089
[29] Abali Y, Bayca S, Mistincik E. Kinetics of oxalic acid leaching of tincal. Chem Eng J. 2006;123:25–30. doi:10.1016/j.cej.2006.07.012
[30] Tunc M, Yapici S, Kocakerim M, et al. The dissolution kinetics of ulexite in sulphuric acid solutions. Equilibrium. 2001;3(2):175–180.
[31] Mazet N. Modeling of gas-solid reactions. 2. nonporous solids. Int Chem Eng. 1992;32:271–284.
[32] O L. Chemical Reaction Engineering1999.
[33] Abanades S, Kimura H, Otsuka H. Kinetic investigation of carbon-catalyzed methane decomposition in a thermogravimetric solar reactor. Int J Hydrogen Energy. 2015;40:10744–10755. doi:10.1016/j.ijhydene.2015.07.023
[34] Naktiyok J, Bayrakçeken H. Kinetics of thermal decomposition of phospholipids obtained from phosphate rock. Fuel Process Technol. 2013;116:158–164. doi:10.1016/j.fuproc.2013.05.007
[35] Kuşlu S, Dişli FÇ, Çolak S. Leaching kinetics of ulexite in borax pentahydrate solutions saturated with carbon dioxide. J Ind Eng Chem. 2010;16:673–678. doi:10.1016/j.jiec.2010.07.020